Temporal dynamics of neural activity underlying unconscious processing of manipulable objects

Suzuki,Megumi
Noguchi,Yasuki
Kakigi,Ryusuke

(Citation)
Cortex,50:100-114

(Issue Date)
2014-01

(Resource Type)
journal article

(Version)
Accepted Manuscript

(URL)
https://hdl.handle.net/20.500.14094/90002607

Temporal dynamics of neural activity underlying unconscious processing of manipulable objects

Megumi Suzuki[a], Yasuki Noguchi[a,*] and Ryusuke Kakigi[b]

[a] Department of Psychology, Graduate School of Humanities, Kobe University, 1-1 Rokkodai-cho, Nada, Kobe, 657-8501, Japan.

[b] Department of Integrative Physiology, National Institute for Physiological Sciences, Myodaiji, Okazaki, Japan.

[*] Corresponding author. Department of Psychology, Kobe University, 1-1 Rokkodai-cho, Nada, Kobe, 657-8501, Japan.
Tel. +1-78-803-5516, Fax. +1-78-803-5589, E-mail: ynoguchi@lit.kobe-u.ac.jp

Brief running title: Unconscious processing of tool images
Number of figures: 5 (with 2 tables)
Number of pages: 35 (including figure legends)

Abstract

The primate visual system is assumed to comprise two main pathways: a ventral pathway for shape and color perception and a dorsal pathway for spatial processing and visuomotor control. Previous studies consistently reported strong activation in the dorsal pathway (especially in the inferior parietal region) induced by manipulable object images such as tools. However, it is controversial whether the dorsal pathway retains this preferential activity to tool images under unconscious perception. In the present study, we used magnetoencephalography (MEG) and investigated spatio-temporal dynamics of neural responses to visible and invisible tool images. A presentation of visible tool images elicited a strong neural response over the parietal regions in the left hemisphere peaking at 400 ms. This response unique to the processing of tool information in the left parietal regions was still observed when conscious perception of tool images was inhibited by interocular suppression. Furthermore, analyses of neural oscillation signals revealed a suppression of μ rhythm (8 – 13 Hz), a neural index of movement execution or imagery, induced by both visible and invisible tools. Those results indicated that the neural circuit to process the tool information was preserved under unconscious perception, highlighting an implicit aspect of the dorsal pathway.

Key words: continuous flash suppression, dorsal visual pathway, magnetoencephalography, subliminal stimuli.

1. Introduction

Many studies have provided considerable evidence for the "unconscious" processing of sensory stimuli in the brain (Dehaene et al., 2006; Fang and He 2005; Sterzer et al., 2009). To elucidate differences in neural mechanisms between conscious and unconscious sensory processing is one of the important themes in neuroscience and psychology (Block 2005; Crick and Koch 2003; Tononi and Edelman 1998).

Previous studies have approached this issue mainly using visual stimuli, partly because of a number of psychophysical techniques to make visual stimuli invisible (Dehaene et al., 2001; Hesselmann and Malach 2011; Jiang and He 2006; Sterzer et al., 2009). In the primate brain, there are two major pathways that receive and process visual information from the retina; the ventral (what) and dorsal (where or how) pathways (Ungerleider and Mishkin 1982). The ventral pathway projects from the primary visual cortex (V1) through the ventral occipital structures to anterior temporal cortex. This pathway is dedicated to processing object identities (Fujita et al., 1992). On the other hand, spatial and visuomotor analyses to grasp and manipulate objects are performed by the dorsal pathway that projects from V1 through the dorsal occipital to posterior parietal cortices (Creem-Regehr and Lee 2005; Milner 2012; Proverbio et al., 2011).

It was suggested that those two pathways have different categories of preferred stimuli. The most well-known stimulus that effectively activates the ventral pathway is faces. Electrophysiological studies using monkeys (Perrett et al., 1985; Tsao et al., 2006) reported that some neurons in the inferior temporal cortex show a particularly strong response to faces than other categories of objects (face-selective neurons). Accordingly, recent studies of fMRI on human subjects (Kanwisher et al., 1997) found brain regions specialized for the processing of face stimuli, such as the occipital face area (OFA) and the fusiform face area (FFA). Another line of studies (Anaki et al., 2007; Eimer 2000; Itier and Taylor 2004;

McCarthy et al., 1999; Miki et al., 2007; Watanabe et al., 2005) using electroencephalography (EEG) and magnetoencephalography (MEG) also reported neural responses from the occipito-temporal regions to face images (face selective N170/M170 in EEG/MEG). Those strong activities for specific categories of objects, however, were limited to visible images consciously perceived. When the stimuli were presented unconsciously, this lack of visual awareness to the stimuli substantially suppressed neural responses in the ventral regions (Lin and He 2009). For example, Pasley et al. used interocular suppression, a psychophysical technique that renders visual stimuli invisible, and reported a near-complete inhibition of neural activities in the inferior temporal cortex to face stimuli unconsciously perceived (Pasley et al., 2004). Although some studies indicated a possibility of residual activities to invisible face stimuli (Jiang and He 2006; Sterzer et al., 2009; Suzuki and Noguchi 2013), those studies overall show a substantial change of neural activities in the ventral regions depending on whether the stimuli are perceived consciously or unconsciously.

In contrast to the ventral pathway, it remains to be elucidated how the lack of conscious percept affects neural activities in the dorsal pathway. Although a classical theory proposed a dichotomy between "what" and "where" (or "how") streams (Ungerleider and Mishkin 1982), more recent studies provided evidence for further anatomical and functional distinctions within the dorsal pathway (Rizzolatti et al., 1998). In a well-known (two-systems) model, the dorsal stream was divided into two sub-pathways; the dorso-dorsal pathway for an online control of action and the ventro-dorsal pathway for skilled action and action recognition (Binkofski and Buxbaum 2012; Buxbaum and Kalenine 2010; Rizzolatti and Matelli 2003). The dorso-dorsal pathway, typically running from the visual area 6 (V6) and the superior parietal lobe (SPL) to the dorsal premotor cortex, processes structural information (size and shape, etc.) of visual stimuli at which actions are directed. This circuit is mainly concerned with the online control and spatio-motor transformations for reaching and

grasping. On the other hand, the ventro-dorsal pathway, projecting from the medial superior temporal area (MST) into inferior parietal lobe (IPL), is related to long-term storage of the skilled actions with familiar objects. This circuit is known to play a major role in tool use.

Consistent with the two-systems model in the dorsal pathway, previous studies showed that viewing tools enhanced neural responses in the inferior parietal regions (Bach et al., 2010; Frey 2007). Additional activities were also observed in motor-related regions including the premotor and somatosensory areas (Chao and Martin 2000; Grafton et al., 1997; Grezes and Decety 2002; Kellenbach et al., 2003), even when no overt actions were required in a task (Creem-Regehr and Lee 2005). Those activities in the inferior parietal and motor-related regions were especially strong in the left hemisphere (Chao and Martin 2000; Creem-Regehr and Lee 2005; Grafton et al., 1997; Grezes and Decety 2002; Kellenbach et al., 2003), which is also a hallmark of the dorso-ventral pathway (Binkofski and Buxbaum 2012). Interestingly, a previous fMRI study reported that those activities in the parietal regions were mostly unchanged even when tool images were made invisible by an interocular suppression (Fang and He 2005). This visibility-invariant property in the dorsal pathway is consistent with a case report of patient D.F. who had a severe bilateral damage in the occipito-temporal areas (Goodale and Milner 1992; Goodale et al., 1991). Despite her inability of discriminating simple geometric shapes, she could use information from objects (e.g. tools) unconsciously to guide her hand movements. Those findings suggest that neural processing in the dorsal pathway is performed implicitly and thus is not available to conscious awareness (Milner 2012). However, another recent study of fMRI provided the data inconsistent with this view (Hesselmann and Malach 2011). Using continuous flash suppression (CFS) (Tsuchiya and Koch 2005), they showed that an inhibition of conscious perception of tool images substantially reduced neural responses in the V1 and dorsal pathway. It is therefore controversial whether the dorsal pathway retains significant neural responses to invisible tool

images.

In the present study, we combined CFS with MEG measurements and examined a role of the dorsal pathway in the processing of invisible tools. There are two advantages of using MEG. First, we could directly measure neural activities related to face and tool perception with a fine temporal resolution. As described above, the brain responses to tool images are characterized by a flow of neural activities from the visual area to the parieto-frontal regions via the dorsal (ventro-dorsal) pathway. Therefore, we investigated whether neural activities in this elemental circuit for tool processing are observed in unconscious as well as conscious perception. Second, the use of MEG enables us to analyze oscillation signals in neural activities. A previous study (Proverbio 2012) reported that conscious perception of tool images (without motor responses) induced a neural desynchronization in upper μ frequency band (10-12 Hz) over centro-parietal sites. If this phenomenon is also observed under unconscious condition in the present study, those results would provide additional evidence for a preservation of the neural circuit to process manipulable objects in unconscious perception.

2. Methods

2.1. Subjects

We recruited 16 subjects for the present experiments. As a result of an initial screening of behavioral data, 5 subjects were excluded because they showed task accuracy higher than chance level even under CFS (invisible condition, see below). Remaining eleven subjects (7 males, age: 20 - 49) participated in two MEG experiments (Exps. 1 and 2). Those two experiments were conducted on the same day, and an order of the two experiments was randomized across subjects. All subjects have normal or corrected-to-normal vision. According to Edinburgh Handedness Inventory (Oldfield 1971), they were strongly

right-handed (a range of Laterality Quotient: 0.8 - 1), except for one (Laterality Quotient: -0.29). Informed consent was received from each subject after the nature of the study had been explained. Approval for the experiment was obtained from the ethics committee of Kobe University, Japan.

2.2. Stimuli and tasks

2.2.1.Experiment 1 (Visible condition)

In Experiment 1, we measured neuromagnetic responses to object images consciously perceived. All visual stimuli were generated using Matlab Psychophysics Toolbox (Brainard 1997; Pelli 1997) and presented on a screen at a refresh rate of 60 Hz. For dichoptic viewing, we presented stimuli at two different locations on the screen. A square area (delineated by white lines, 6.1°×6.1°) on the left half of the screen comprised stimuli for the left eye of the subject, whereas another area on the right half comprised stimuli for the right eye. Stimuli at these two locations were fused using a mirror stereoscope placed in front of the subject's eyes.

We presented subjects with 6 types of images; low-contrast object images of three categories (face, house and tool) and their scrambled (random) images (**Fig.1A**). Mean luminance and RMS contrasts were controlled across the three categories (luminance: 8.88 cd/m^2 for faces, 8.90 cd/m^2 for houses, and 8.89 cd/m^2 for tools, RMS contrasts: 1.41 cd/m^2 for faces, 1.39 cd/m^2 for houses, and 1.40 cd/m^2 for tools). The random images were created by the two-dimensional (2D) Fourier transformation of the low-contrast intact images, and thus contained the same spectra of spatial frequencies as those in the intact images. To control a variety of stimuli across the three categories, we used 6 different images for each category. Faces of 6 persons were taken from the ATR facial expression image database (DB99, ATR promotions, Kyoto, Japan), while intact house images were downloaded from the Internet. For tools, we used the same set of images as previous studies (Almeida et al.,

2008; Mahon et al., 2007) so that the present results could be compared with previous ones. Those contained scissors, broom, knife, fork, racket and wrench.

As described in **Introduction**, our purpose in the present study was to compare neural responses to various objects (especially tools) between visible (Exp. 1) and invisible (Exp. 2) conditions. To make the objects images visible to subjects, we presented a uniform gray screen (instead of continuous flashes) to dominant eyes of subjects in Experiment 1 (**Fig. 1B**). Every trial consisted of two successive temporal intervals (1.3 s for each, with a 500-ms blank gap between them). Each interval began with a gray screen with a fixation point to both eyes for 0.6 s, followed by an image (intact or random image of object) to a non-dominant eye for 0.5 s. The interval ended with the gray fixation screen to both eyes for 0.2 s. There were three types of trials (face, house, and tool trials) in Experiment 1. In the face trial, an intact face image was presented in either the first or second interval randomly determined, while its random (scrambled) image was given in the other interval. Likewise, an intact house (tool) image was paired with its random version in the house (tool) trials. Those three types of trials were randomly intermixed in an experimental session of 72 trials (24 trials for each). The task of subjects was to report the category of the intact image (face, house or tool) by pressing one of three buttons (discrimination task), neglecting the random image in the other interval. Each subject performed two sessions (144 trials in total).

2.2.2. Experiment 2 (Invisible condition)

In Experiment 2, we measured neuromagnetic responses to invisible object images using continuous flash suppression (CFS). A structure of one trial was same as Experiment 1, except that we presented continuous flashes to dominant eye of subjects to make object images (to non-dominant eye) invisible (**Fig. 3A**). In each interval of 1.3 s, a rapid sequence of 26 colored Mondrian patterns was presented to dominant eye. Those continuous flashes

were also given to non-dominant eye at the last 0.2 s of each interval, to avoid afterimages generated from the intact or random objects.

In addition to the 6 types (face/house/tool × intact/random) of images in Experiment 1, we newly employed two conditions, high-contrast and gray ones. In the high-contrast condition, we presented an intact image of a face, house or tool with a higher luminance contrast. Because of the higher contrast, subjects consciously perceived the object images even during the presentation of continuous flashes. This condition of high-contrast images were employed to ascertain and maintain the subjects' motivation for the tasks (Sterzer et al., 2009). In the gray condition, we presented a uniform gray screen instead of the intact or random object image. The MEG waveforms of this condition should contain neural responses to continuous flashes but not responses to target objects, thus serving as the lowest control condition to isolate neural responses to the object images. Those high-contrast and gray stimuli were paired as the first and second images within the same trial, which formed the fourth type of trial (the high-gray trial). A total of 4 types of trials (face, house, tool, and high-gray) were randomly intermixed in an experimental session of 72 trials (18 for each). One experiment comprised 4 sessions.

Subjects were asked to perform two tasks in every trial. In the first task, they reported the interval (1st or 2nd) in which the intact image, not random image, was presented. This two-alternative forced-choice (2AFC) task is known to be the most sensitive way to probe visibility of the stimuli (Sterzer et al., 2009). In the second task, subjects reported the category (face, house or tool) of the intact object that was presented at either first or second interval (discrimination task).

2.3. MEG measurements

Visual-evoked fields (VEFs) to the intact, random as well as high-contrast object images were

measured using a whole-head 306-channel MEG system (Vector-view, ELEKTA Neuromag, Helsinki, Finland), which recorded changes in neuromagnetic signals from 102 different positions over the scalp. A sensor element at each recording position consisted of one magnetometer and two orthogonal planer-type gradiometers (one for measuring latitudinal and the other for measuring longitudinal directions of changes in neuromagnetic signals). In the present study, we analyzed MEG signals recorded from 204 gradiometers at 102 sensor positions. The signals from the planar-type gradiometers are strongest when the sensors are located just above local cerebral sources (Nishitani and Hari 2002). The measurements were performed with a band-pass filter of 0.1-200 Hz at a sampling rate of 1000 Hz. For each of the 6 (Exp. 1) or 8 (Exp. 2) conditions above, neuromagnetic waveform in 48 (Exp. 1) or 72 (Exp. 2) trials at maximum were averaged to yield a VEF in that condition. An epoch for the averaging ranged from -700 to 800 ms relative to the onset of the object images, with -100 to 0 ms used as a baseline. Trials in which signal variations were larger than 3000 fT/cm were excluded from analysis.

To evaluate the strength of neural responses at each of 102 sensor positions, we integrated neuromagnetic signals (VEFs) recorded from two types of planar sensors (gradiometers). This integration was performed by calculating a vector norm (root sum square) of the two gradiometers at each sensor position, as shown in an equation below (Noguchi et al., 2012)

$$\sqrt{x_i^2 + y_i^2}$$

, where x and y indicated MEG signals (fT/cm) in the latitudinal (x) and longitudinal (y) gradiometers at the sensor position i (1-102). Note that, after the transformation into those vector norm values, strong neuromagnetic responses are shown as upward deflections of the VEF waveforms. To identify neural responses related to object recognition in high-level

(not low-level) visual regions, we then compared VEFs to the intact objects with those to the random images. Differential VEFs between the intact and random conditions were acquired for each of three categories (face, house and tool, **Fig. 2A**). See **Supplementary Fig. S1** and **Fig. S2** for non-differential VEFs to intact and random images.

2.4. Sensor of interest analyses

Although we recorded neural activity from the whole brain of subjects, the purpose of the present study was to investigate neural responses to visible and invisible objects images. The main regions of interest therefore were the high-level (extrastriate) visual areas in the dorsal and ventral pathways related to the processing of visual objects. To focus on the neural signals emerging from those high-level visual cortices, we took the sensor of interest (SOI) approach in the previous MEG studies (Furey et al., 2006; Liu et al., 2002; Noguchi et al., 2004).

First, we averaged the differential (intact – random) VEFs to visible face and tool images in Experiment 1. The differential waveforms to the house images were not used in the SOI analyses, because the MEG responses to the house images were substantially weaker than those in the face and tool conditions even when the houses were visible to subjects (see **Results** and **Fig. 2**). Using those averaged (F+T) waveforms, we selected the SOIs in the present study based on the following criteria: a positive peak deflection in the F+T waveforms was observed in a time window of 0-500 ms after the onset of the object images, and a significant deflection (> 2 SD of the fluctuations in a baseline (from -100 to 0 ms) period of each channel) continued for at least 30 ms centering on the peak latency (Noguchi et al., 2004). An average of 32.1 SOIs (out of all 102 sensor positions) was selected for each subject. Spatial distributions of those SOIs were shown in **Figure 4A**. We then divided these SOIs into two hemispheric groups (left SOIs and right SOIs), depending on the location

of the SOIs on the scalp. This left-right separation of the MEG data was based on the hemispheric dominance in the processing of face and tool images. First, it is known that the information of tool images is mainly processed in the left hemisphere (Andres et al., 2012; Chao and Martin 2000; Creem-Regehr and Lee 2005; Grafton et al., 1997; Grezes and Decety 2002; Kellenbach et al., 2003; Vingerhoets et al., 2013). Second, a recent study showed that N170 responses to face stimuli were lateralized into the right hemisphere in male brain while those were bilateral in female brain (Proverbio et al., 2010). Given a high percentage of male subjects in the present study (64 %), it is possible that neuromagnetic responses to face images were larger in the right than left hemispheres. The 6 sensors on midline regions were excluded from further analyses (see dotted rectangle in **Fig. 1C**). Using this SOI information, we then averaged differential (intact - random) VEFs across all SOIs within each hemispheric group, producing an across-SOI VEFs for each hemisphere. The across-SOI VEFs were then baseline-corrected using the data at -100 to 0 ms. This averaging of VEFs across SOIs was performed for each of 4 conditions in Experiments 1 and 2 (face/tool × visible/invisible, **Fig. 4B**).

Using the across-SOI VEFs of 11 subjects, we compared neuromagnetic responses to face and tool stimuli at the population level. First, we divided the across-SOI VEFs of each subject from 50 - 750 ms into 7 time windows of 100 ms (Rotshtein et al., 2010; Yokoyama et al., 2013), and obtained a mean amplitude of neuromagnetic responses within each time window. For each of visible and invisible condition, a three-way ANOVA was then performed (**Fig. 4B** and **Fig. 4C**) where this factor of 7 time windows (50-150 ms, 150-250 ms, 250-350 ms, 350-450 ms, 450-550 ms, 550-650 ms, 650-750 ms) were combined with factors of object category (face/tool) and hemisphere (left/right).

2.5. Distributed source estimations of neuromagnetic signals

In addition to the SOI analysis, we estimated source locations of MEG signals using Statistical Parametric Mapping 5 (SPM5, available on-line at www.fil.ion.ucl.ac.uk/spm/). Three-dimensional source reconstructions of MEG signals were performed by the multiple sparse priors (MSP) approach (Friston et al., 2008). First, the VEFs in all conditions were low-pass-filtered at 30 Hz and down-sampled to 200 Hz. A tessellated cortical mesh was then created for each subject using a template brain from the Montreal Neurological Institute (MNI). This mesh contained 7200 vertices and served as a model brain to estimate current source distributions. Positions of current dipole mesh were restricted to a cortical surface, and they were evenly placed at each node of the mesh. This dipole mesh was spatially coregistered with a sensor space of MEG, based on digitized locations of the nasion and bilateral peri-auricular points of each subject (Henson et al., 2007). We then constructed a single-shell, spherical head model for forward solutions, as implemented in BrainStorm (available on-line at neuroimage.usc.edu/brainstorm). Finally, the forward model was inverted with the MSP approach, which mapped the contribution (source strength) of each dipole on the mesh to MEG sensor waveforms. We performed these MSP estimations for each time point, trial, and subject.

For second-level (group-level) analysis across the 11 subjects, the MSP solutions for each trial and each subject were averaged over all time points belonging to a time window of interest. For the face stimuli in the visible condition, this time window was set at 150-230 ms (**Fig. 4B right**), conforming to previous EEG and MEG studies on the N170 (M170) responses to face images (Sadeh and Yovel 2010; Sterzer et al., 2009). For visible and invisible tool images, the time windows were set at 350-450 ms and 650-750 ms, respectively, based on the results of three-way ANOVAs (time × object category × hemisphere) on the across-SOI VEFs (see **Sensor of interest analyses** and **Results**). The resultant MSP

estimations (averaged across the time window of interest) were then analyzed by SPM random-effect analysis (Henson et al., 2007). Differences between trials (e.g. intact face vs. random face) were evaluated by voxel-wise *t* tests of SPM5. The threshold for a significant difference was set at FDR (false discovery rate) corrected $p = .01$.

2.6. Frequency analyses of neuromagnetic waveforms

In addition to the VEF analyses, we also investigated neural oscillation signals when subjects perceived visible and invisible tool images. It is known that neural activity of the motor and somatosensory cortices during action observation, imitation and execution induce a desynchronization of the μ rhythm of 8-13 Hz (Matsumoto et al., 2010). A recent study further showed a suppression of upper μ rhythm of 10-12 Hz during an observation of visible tool images even when no overt actions were required in a task (Proverbio 2012). We thus tested whether the desynchronization in upper μ rhythm was also seen in unconscious processing of tool images.

Procedures of frequency analyses conformed to those in previous studies (Osipova et al., 2005; Piitulainen et al., 2013; Pohja et al., 2005). First, continuous MEG waveforms in each sensor were split into 512 ms epochs with a 504-ms overlap between contiguous epochs. Those segmented waveforms were then converted into power spectra using the fast Fourier transform, and averaged across 48 (visible) or 72 (invisible) trials. As analyses of the VEFs, the data in the random image condition was subtracted from the intact image condition to isolate neural signals related to object perception. Finally, we performed the across-sensor averaging of those power spectra. Since the desynchronization of the μ rhythm is usually seen over the sensorimotor regions along the central sulcus, we selected 11 sensors in **Figure 1C** (see a region encompassed by red lines) as the SOIs (sensors of interest) for the frequency analyses. This selection was based on distinct neural responses to visible and invisible tool

images observed in the left hemisphere (see **Results**) and results of our previous studies investigating MEG waveforms during somatosensory stimulations and executions of finger movements (Kida et al., 2006; Nakata et al., 2009; Wasaka et al., 2003). Those 11 sensor positions are located near the C3 electrode in the international 10-20 system. We averaged the differential (intact - random) power spectra in the 11 SOIs and produced across-SOI spectra for visible and invisible tool images (**Fig. 5A**). The temporal changes of the power in the upper μ band were then averaged across all subjects (**Fig. 5B**).

A previous study (Proverbio 2012) reported that the desynchronization in upper μ rhythm to tool images was observed earlier (by up to 130 ms) than an onset of visual-evoked potential (VEPs) to the same images. Given that we observed the distinct VEFs to invisible tools at 650-750 ms (see **Results**), an expected time period for the decrease in μ power would be at around 520-620 ms. We thus averaged power spectra within a time window of 520-620 ms, and compared it with the spectra at 0 ms (baseline period). If the presentation of invisible tools induced the desynchronization, a significant difference in upper μ power should be observed between those two.

3. Results

3.1. Experiment 1

In Experiment 1, we presented subjects with object images that could be perceived consciously (visible condition). Mean (± SE across subjects) accuracy of the discrimination task (face, house, or tool, chance level: 33.3 %) was 99.6 ± 0.1 %, indicating that the intact and random images in Experiment 1 were actually visible to subjects. We then investigated neural activity induced by those visible stimuli. To focus on neural responses for recognition of objects (not a perception of low-level visual features), we subtracted VEFs to the random images from those to the intact objects. **Figure 1C** shows those differential VEFs to visible

faces for one subject over 102 sensor positions of MEG. We enlarged VEFs at two sensor positions, one in the right and another in the left hemispheres (**Fig. 1D**). The differential (intact – random) VEFs to face, house, and tool images are shown in red, green, and blue lines, respectively. Note that, since we showed VEFs being transformed into vector norm values, strong neural responses are represented as upward deflections of the VEFs. To obtain an overview of VEFs at 102 sensors, we divided those into 26 groups (4 sensors per group, except for one group of 2 sensors at the most anterior-midline position over the medial frontal cortex). The VEFs at 4 (or 2) sensors belonging to the same group were averaged together. The resultant VEFs in the 26 groups (averaged across all subjects) were displayed in **Figure 2A**. Clear responses to faces (red) were observed in the occipito-temporal regions in the right hemisphere, while the tool images (blue) elicited strong neural activity in the left hemisphere (orange circles). On the hand, we found that neural responses for house images were quite weak. **Figure 2B** shows peak amplitudes of VEFs over the 26 sensor groups. We identified a peak amplitude of VEF in each sensor group (within a time window of 0 -800 ms) and averaged it across the 26 groups. One-way ANOVA indicated a significant main effect of object categories (face/house/tool, $F(2,20) = 8.70$, $p = .002$). Post-hoc tests with Bonferroni corrections indicated significant differences in face versus house ($p = .022$) and house versus tool ($p = .047$), but not in face versus tool ($p = .24$). This reduction in VEF amplitudes to house images might be related to the fact that the brain areas strongly reacting to house stimuli (house regions) are located in medial regions of the ventral pathway near the bottom of the brain (Epstein and Kanwisher 1998; Konkle and Oliva 2012). Since magnetic signals detected by an MEG sensor decreases as a distance from a signal source (in the cerebral cortex) to the MEG sensor becomes larger, the medial locations of the house regions might lower a sensitivity of the present MEG measurements to the house stimuli, resulting in the smaller amplitudes of VEFs to the houses than face and tool images. We thus excluded

these VEFs to house images from further analyses.

3.2. Experiment 2

In Experiment 2, we presented the same set of object images as Experiment 1 under continuous flash suppression, so that subject could not perceive those images consciously. **Figure 3B** shows the behavioral data in two tasks of Experiment 2. In the first task (the 2AFC detection task), subjects reported which interval (1st or 2nd) contained an intact object image. When high-contrast object images were presented, mean (± SE) detection rate was 93.1 ± 3.5 %, significantly larger than chance level of 50 % ($t(10) = 12.3$, $p < .001$). On the other hand, the detection rate of low-contrast images was 50.5 ± 3.1 % and there was no significant difference from chance level ($t(10) = .16$, $p = .871$). The detection rate for low-contrast face, house and tool images were 51.3 ± 2.8 %, 49.2 ± 3.3 % and 50.9 ± 4.1 %, respectively. No difference in the detection rates was observed across the three object categories (a main effect of one-way ANOVA; $F(2,20) = 0.32$, $p = .73$. In the second task (discrimination task), subjects reported a category of the intact object (face, house or tool). Similar to the detection task, a discrimination rate of high-contrast images was 84.3 ± 4.7 %, significantly higher than chance level of 33 % ($t(10) = 10.9$, $p < .001$). The discrimination rate of the low-contrast images was 36.9 ± 1.7 %, which showed a tendency of a significant difference from the chance level ($t(10) = 2.1$, $p = .061$). No difference in the discrimination rate was observed across the three categories (face: 38.4 ± 6.2 %, house: 38.0 ± 4.2 %, tool: 34.3 ± 3.0 %, a main effect of one-way ANOVA; $F(2,20) = 0.19$, $p = .83$). One group *t*-tests revealed no significant difference from chance level (33 %) in any categories (face: $t(10) = 0.82$, $p = .43$, house: $t(10) = 1.13$, $p = .29$, tool: $t(10) = 0.31$, $p = .76$). Those behavioral data overall indicated that low-contrast images were kept invisible under CFS, while a presentation of high-contrast images broke the perceptual suppression and entered into consciousness of

subjects. The differential (intact – random) VEFs to those invisible (low-contrast) objects were shown in **Figure 3C**. As **Figure 2A**, the VEFs at 102 sensors were classified into 26 groups and waveforms within each group were averaged. Some neuromagnetic responses especially to tools were seen in the left hemisphere (orange circles), although amplitudes of those VEFs to invisible objects were generally smaller than those to visible objects in Experiment 1.

3.3. Comparisons of MEG responses between the visible and invisible conditions

We took the SOI (sensor of interest) approach (see **Methods** for details) to focus on neuromagnetic responses from the high-level (extrastriate) visual areas in the dorsal and ventral pathways related to the processing of visual objects. In this approach, a subset of MEG sensors (SOIs) were first selected for each subject that showed greater responses to intact than random images of objects. We chose SOIs in the present study using VEFs to visible face and tool stimuli in Experiment 1 (**Fig. 2A**). **Figure 4A** shows spatial distributions of those SOIs. This map represents how many times each sensor was selected across 11 subjects (the position of a sensor was colored red when this sensors was selected as SOI in many subjects). Consistent with our previous studies, most SOIs concentrated in the occipito-temporal regions in both hemispheres (Noguchi et al., 2004), which reflected objected-selective (intact > random) responses in the ventral visual pathway. In the left hemisphere, the second center was seen at a position anterior to the occipito-temporal source. No sensor around the occipital pole (over the early visual regions such as the V1) was selected as SOIs.

Using this SOI information as a localizer for the object-selective visual regions, we averaged differential (intact - random) VEFs in the 4 conditions (visible/invisible × face/tool) across all SOIs. This across-SOI averaging was conducted for each hemisphere. **Figure**

4B shows those across-SOI VEFs (mean of 11 subjects) of left and right hemispheres in the visible condition. A three-way ANOVA (face/tool × 7 time windows × left/right hemispheres, see **Methods**) indicated significant main effects of object category (face > house, $F(1,270) = 5.18$, $p = .024$) and time ($F(6,270) = 10.78$, $p < .001$) as well as a significant interaction of category and time ($F(6,270) = 2.84$, $p = .011$). No other main effect or interaction was observed ($p > .08$ for all). To analyze the category-time interaction in detail, we applied a two-way ANOVA (category × time) for the data in each hemisphere. In the left hemisphere (**Fig. 4B**, left), we found significant a main effect of time ($F(6,130) = 4.33$, $p = .001$) and a category × time interaction ($F(6,130) = 3.51$, $p = .003$), with a non-significant main effect of category ($F(1,130) = 0.139$, $p = .71$). Post-hoc comparisons revealed larger MEG responses to faces than tools at 150-250 ms ($p = .01$) and 650-750 ms ($p = .018$), and a larger response to tools than faces at 350-450 ms ($p = .019$). On the other hand, a two-way ANOVA in the right hemisphere (**Fig. 4B**, right) showed significant main effects of category (faces > tools, $F(1,130) = 8.57$, $p = .004$) and time ($F(6,130) = 6.98$, $p < .001$) with a non-significant category × time interaction ($F(6,130) = 0.805$, $p = .57$). Those results indicated that, although visible face images induced stronger neuromagnetic responses than visible tool images (as shown by the significant main effect of category in the three-way ANOVA), the tool images evoked distinct neural activity especially in the left hemisphere at 350-450 ms, resulting in the significant category × time interaction.

Figure 4C shows the across-SOI VEFs (mean of 11 subjects) in the invisible condition. The three-way ANOVA (category × time × hemisphere) yielded no significant main effect or interaction ($p > .062$ for all) except for a significant interaction between category and hemisphere ($F(1,270) = 9.02$, $p = .003$). The two-way ANOVA in the left hemisphere indicated a significant main effects of category (tool > face, $F(1,130) = 12.97$, $p < .001$), while no main effect of time ($F(6,130) = 1.26$, $p = .28$) or category × time interaction

($F(6,130) = 1.16$, $p = .34$) was observed. On the other hand, there was no main effect or interaction in the right hemisphere (main effect of category: $F(1,130) = 0.60$, $p = .44$, main effect of time: $F(6,130) = 0.25$, $p = .96$, category × time interaction: $F(6,130) = 0.21$, $p = .97$). Those results showed that the significant category × hemisphere interaction observed in the three-way ANOVA mainly resulted from the larger neural responses to tools than faces in the left hemisphere. One should note that this tool-selective response in the left hemisphere reflected an increased MEG response to intact compared to random tool images, rather than a decreased MEG response to intact compared to random face images. When the across-SOI VEFs to invisible tools were compared from baseline (zero-level), mean amplitude in a time window of 650-750 ms showed a positive deflection from the baseline ($t(10) = 2.79$, $p = .019$). Overall, our analyses on the across-SOI waveforms indicated strong neural responses to tool images in the left hemisphere that was preserved even during a suppression of conscious perception (invisible condition).

Some might argue that the MEG responses in the left hemisphere to invisible tools reflected residual visibility of those images, because the behavioral discrimination rates to those low-contrast tool images were slightly higher (34.3 ± 3.0 %) than the chance level (33 %, see above). We confirmed, however, that those discrimination rates to invisible tools were never correlated with amplitudes of the tool-selective activity in the left hemisphere at 650-750 ms ($r(10) = .066$, $p = .85$) or at 50-750 ms ($r(10) = .34$, $p = .30$). The significant VEFs to invisible tools thus represented unconscious neural processing of tool information, rather than the residual visibility of the low-contrast tool images under CFS.

We estimated source locations for those MEG responses using the MSP analyses on SPM5 (see **Distributed source estimations of neuromagnetic signals**). At 150-230 ms, a presentation of visible face images evoked significant neural responses in various areas including the occipito-temporal regions in the ventral pathway (**Fig. 4B,** right). Based on the

results of ANOVAs (see above), source estimations for visible and invisible tool images were performed at 350-450 ms and 650-750 ms, respectively. Significant responses to visible tool images were found bilaterally in the supramarginal gyrus, superior temporal gyrus, etc (**Fig. 4B**, left). Those responses to tools in the dorsal regions were still observed in the invisible condition, especially in the left hemisphere (**Fig. 4C**). Detailed information about the results of the MSP estimations was shown in **Tables 1 and 2**.

3.4. Desynchronization of upper μ rhythm in perception of invisible tools

Finally, we performed frequency analyses of neuromagnetic waveforms when subjects perceived tool images. The fast Fourier transformation (FFT) was applied to MEG waveforms to visible and invisible tool images (see **Methods**). **Figure 5A** shows time-frequency power spectra averaged across all SOIs in the left hemisphere. In the visible condition (upper panel), we observed a desynchronization of neural activities in an upper μ band (11-13 Hz) beginning from 200 ms after the stimulus onset, which was consistent with a previous study (Proverbio 2012). This suppression of μ rhythm was also seen in invisible condition but in a later time window around 500 ms (lower panel in **Fig. 5A**). As shown in **Figure 5B**, the desynchronization to invisible tool images compared to the baseline period (at 0 ms, see **Methods**) were statistically significant ($t(10) = 2.31$, $p = .044$). Those results indicate that the suppression of μ rhythm, an index of neural activity in the motor and somatosensory cortices, was induced both by visible and invisible tools.

4. Discussion

In the present study, we investigated temporal dynamics of neural responses to various objects such as faces, houses and tools. Of particular interest were responses in the dorsal (ventro-dorsal) pathways to manipulable objects (tools) in conscious and unconscious

conditions. Behavioral results showed that low-contrast object images were visible in Experiment 1 but made invisible by CFS in Experiment 2. When visible face images were presented to subjects, large neural responses were observed in the occipito-temporal regions, which would correspond to N170m or M170 in previous studies (Bentin et al., 1996; Rossion et al., 2003). We found that those neural responses to faces were substantially reduced in the invisible condition. On the other hand, a presentation of visible tool images induced neural activities in the right hemisphere around 200 ms (Proverbio et al., 2011), followed by a strong response in the left hemisphere around 400 ms. The response in the left parietal regions unique to the processing of tool information was also seen in the invisible condition.

4.1. Different latency of neural activity between visible and invisible conditions

We presently compared neural responses in two main conditions; the invisible condition where conscious perception of an object image was inhibited by CFS and the visible condition where no continuous flash but the object image was presented. Since those structures in the visible and invisible conditions were identical to previous studies on unconscious processing of visual objects (Fang and He 2005; Jiang et al., 2009; Sterzer et al., 2009), our results could be directly compared to those previous studies (except that we mainly performed an sensor of interest approach on neuromagnetic waveforms). On the other hand, one should note that there were some differences in experimental procedures between the visible and invisible conditions. For example, continuous flashes were presented to dominant eye of subjects in the invisible condition while not in the visible condition. Those procedural differences between the two conditions might cause some qualitative changes in our MEG waveforms.

For example, we observed significant neural responses to visible tools in the left hemisphere at 350-450 ms after the stimulus onset (**Fig. 4B**). The strong response to tools, however, appeared around 650-750 in the invisible condition (**Fig. 4C**). This delay of neural

latency in the invisible compared to visible conditions were also reported by previous studies using CFS (Jiang and He 2006; Suzuki and Noguchi 2013). Although a precise reason is unclear, one possible reason for this delay would be a lowered excitability of neurons in the visual cortex (Noguchi et al., 2012). Because we presented a sequence of continuous flashes for 600 ms before an onset of object images, those colorful flashes must have strongly activated neurons in the visual area, inducing a habituation (a decrease in excitability) of those neurons. This lowered excitability in the visual area might delay MEG responses to subsequent object images, resulting in an extension of the neural latency in the invisible compared to visible conditions.

4.2. Neural responses to invisible tools in the dorsal pathway

As described in **Introduction**, there was a controversy about how the lack of conscious percepts of tool images affects the neural activities in the dorsal pathway. Some studies reported a large decrease in neural activity to invisible tool images (Hesselmann and Malach 2011; Kaunitz et al., 2011) while others not (Fang and He 2005). In the present study, we observed a strong suppression of neuromagnetic responses to invisible compared to visible images, which was consistent with the results by Hesselmann and Malach (2011). Significant neural responses to invisible tool images were, however, still seen in the left (650 - 750 ms) hemispheres (**Fig. 4C**). Because these significant responses were not observed in invisible face condition, our results suggest that neural processing of the tool information in the dorsal pathway was relatively preserved compared to the face processing in the ventral stream. In this sense, the present data were also consistent with the idea from previous neuropsychological study (Milner 2012).

These neural activities under unconscious processing of tool images were also supported by the results of frequency analyses. The μ rhythm is a neural oscillation

appearing around the central sulcus during a relaxed state. A desynchronization of this rhythm is an index of movement execution and motor imagery (Matsumoto et al., 2010; Proverbio 2012). Although a previous study reported the suppression of μ rhythm induced by visible tool images, we found that this phenomenon occurred even when tool images were perceived unconsciously (**Fig. 5B**). Those results of frequency analyses reinforce our data of VEFs (**Fig. 4**) and provide additional evidence for significant brain responses to invisible tools (Fang and He 2005).

5. Conclusions

In summary, we observed significant neural responses in the human brain to invisible as well as visible tool images. Those responses to invisible tools were clearly seen in the left hemisphere, which suggest an involvement of the dorso-ventral pathway concerned with skilled manipulation of familiar objects (Binkofski and Buxbaum 2012; Buxbaum and Kalenine 2010). Given a limited spatial resolution of our MEG measurements, however, further studies would be necessary to reveal full details of a neural circuit to process the information of invisible tools.

Acknowledgments

This work was supported by KAKENHI Grants Number 22680022 from the Japan Society for the Promotion of Science (JSPS) to Y.N. We thank Mr. Y. Takeshima (National Institute for Physiological Sciences, Japan) for his technical supports.

References

Almeida J, Mahon BZ, Nakayama K, and Caramazza A. Unconscious processing dissociates along categorical lines. *Proceedings of the National Academy of Sciences of the United States of America*, 105(39): 15214-8, 2008.

Anaki D, Zion-Golumbic E, and Bentin S. Electrophysiological neural mechanisms for detection, configural analysis and recognition of faces. *Neuroimage*, 37(4): 1407-16, 2007.

Andres M, Pelgrims B, and Olivier E. Distinct contribution of the parietal and temporal cortex to hand configuration and contextual judgements about tools. *Cortex*, 2012.

Bach P, Peelen MV, and Tipper SP. On the role of object information in action observation: an fMRI study. *Cerebral Cortex*, 20(12): 2798-809, 2010.

Bentin S, Allison T, Puce A, Perez E, and McCarthy G. Electrophysiological Studies of Face Perception in Humans. *Journal of Cognitive Neuroscience*, 8(6): 551-65, 1996.

Binkofski F and Buxbaum LJ. Two action systems in the human brain. *Brain and Language*, 2012.

Block N. Two neural correlates of consciousness. *Trends in Cognitive Sciences*, 9(2): 46-52, 2005.

Brainard DH. The Psychophysics Toolbox. *Spatial Vision*, 10(4): 433-6, 1997.

Buxbaum LJ and Kalenine S. Action knowledge, visuomotor activation, and embodiment in the two action systems. *Annals of The New York Academy of Sciences*, 1191: 201-18, 2010.

Chao LL and Martin A. Representation of manipulable man-made objects in the dorsal stream. *Neuroimage*, 12(4): 478-84, 2000.

Creem-Regehr SH and Lee JN. Neural representations of graspable objects: are tools special? *Brain Research Cognitive Brain Research*, 22(3): 457-69, 2005.

Crick F and Koch C. A framework for consciousness. *Nature Neuroscience*, 6(2): 119-26, 2003.

Dehaene S, Changeux JP, Naccache L, Sackur J, and Sergent C. Conscious, preconscious, and subliminal processing: a testable taxonomy. *Trends in Cognitive Sciences*, 10(5): 204-11, 2006.

Dehaene S, Naccache L, Cohen L, Bihan DL, Mangin JF, Poline JB, and Riviere D. Cerebral mechanisms of word masking and unconscious repetition priming. *Nature Neuroscience*, 4(7): 752-8, 2001.

Eimer M. Effects of face inversion on the structural encoding and recognition of faces. Evidence from event-related brain potentials. *Brain Research Cognitive Brain Research*, 10(1-2): 145-58, 2000.

Epstein R and Kanwisher N. A cortical representation of the local visual environment. *Nature*, 392(6676): 598-601, 1998.

Fang F and He S. Cortical responses to invisible objects in the human dorsal and ventral pathways. *Nature Neuroscience*, 8(10): 1380-5, 2005.

Frey SH. What puts the how in where? Tool use and the divided visual streams hypothesis. *Cortex*, 43(3): 368-75, 2007.

Friston K, Harrison L, Daunizeau J, Kiebel S, Phillips C, Trujillo-Barreto N, Henson R, Flandin G, and Mattout J. Multiple sparse priors for the M/EEG inverse problem. *Neuroimage*, 39(3): 1104-20, 2008.

Fujita I, Tanaka K, Ito M, and Cheng K. Columns for visual features of objects in monkey inferotemporal cortex. *Nature*, 360(6402): 343-6, 1992.

Furey ML, Tanskanen T, Beauchamp MS, Avikainen S, Uutela K, Hari R, and Haxby JV. Dissociation of face-selective cortical responses by attention. *Proceedings of the National Academy of Sciences of the United States of America*, 103(4): 1065-70, 2006.

Goodale MA and Milner AD. Separate visual pathways for perception and action. *Trends in Neurosciences*, 15(1): 20-5, 1992.

Goodale MA, Milner AD, Jakobson LS, and Carey DP. A neurological dissociation between perceiving objects and grasping them. *Nature*, 349(6305): 154-6, 1991.

Grafton ST, Fadiga L, Arbib MA, and Rizzolatti G. Premotor cortex activation during observation and naming of familiar tools. *Neuroimage*, 6(4): 231-6, 1997.

Grezes J and Decety J. Does visual perception of object afford action? Evidence from a neuroimaging study. *Neuropsychologia*, 40(2): 212-22, 2002.

Henson RN, Mattout J, Singh KD, Barnes GR, Hillebrand A, and Friston K. Population-level inferences for distributed MEG source localization under multiple constraints: application to face-evoked fields. *Neuroimage*, 38(3): 422-38, 2007.

Hesselmann G and Malach R. The link between fMRI-BOLD activation and perceptual awareness is "stream-invariant" in the human visual system. *Cerebral Cortex*, 21(12): 2829-37, 2011.

Itier RJ and Taylor MJ. N170 or N1? Spatiotemporal differences between object and face processing using ERPs. *Cerebral Cortex*, 14(2): 132-42, 2004.

Jiang Y and He S. Cortical responses to invisible faces: dissociating subsystems for facial-information processing. *Current Biology*, 16(20): 2023-9, 2006.

Jiang Y, Shannon RW, Vizueta N, Bernat EM, Patrick CJ, and He S. Dynamics of processing invisible faces in the brain: automatic neural encoding of facial expression information. *Neuroimage*, 44(3): 1171-7, 2009.

Kanwisher N, McDermott J, and Chun MM. The fusiform face area: a module in human extrastriate cortex specialized for face perception. *The Journal of Neuroscience*, 17(11): 4302-11, 1997.

Kaunitz LN, Kamienkowski JE, Olivetti E, Murphy B, Avesani P, and Melcher DP. Intercepting the First Pass: Rapid Categorization is Suppressed for Unseen Stimuli. *Frontiers in Psychology*, 2: 198, 2011.

Kellenbach ML, Brett M, and Patterson K. Actions speak louder than functions: the importance of manipulability and action in tool representation. *Journal of Cognitive Neuroscience*, 15(1): 30-46, 2003.

Kida T, Wasaka T, Inui K, Akatsuka K, Nakata H, and Kakigi R. Centrifugal regulation of human cortical responses to a task-relevant somatosensory signal triggering voluntary movement. *Neuroimage*, 32(3): 1355-64, 2006.

Konkle T and Oliva A. A real-world size organization of object responses in occipitotemporal cortex. *Neuron*, 74(6): 1114-24, 2012.

Lin Z and He S. Seeing the invisible: the scope and limits of unconscious processing in binocular rivalry. *Progress in Neurobiology*, 87(4): 195-211, 2009.

Liu J, Harris A, and Kanwisher N. Stages of processing in face perception: an MEG study. *Nature Neuroscience*, 5(9): 910-6, 2002.

Mahon BZ, Milleville SC, Negri GA, Rumiati RI, Caramazza A, and Martin A. Action-related properties shape object representations in the ventral stream. *Neuron*, 55(3): 507-20, 2007.

Matsumoto J, Fujiwara T, Takahashi O, Liu M, Kimura A, and Ushiba J. Modulation of mu rhythm desynchronization during motor imagery by transcranial direct current stimulation. *Journal of NeuroEngineering and Rehabilitation*, 7: 27, 2010.

McCarthy G, Puce A, Belger A, and Allison T. Electrophysiological studies of human face perception. II: Response properties of face-specific potentials generated in occipitotemporal cortex. *Cerebral Cortex*, 9(5): 431-44, 1999.

Miki K, Watanabe S, Honda Y, Nakamura M, and Kakigi R. Effects of face contour and features on early occipitotemporal activity when viewing eye movement. *Neuroimage*, 35(4): 1624-35, 2007.

Milner AD. Is visual processing in the dorsal stream accessible to consciousness? *Proceedings of the Royal Society B: Biological Sciences*, 279(1737): 2289-98, 2012.

Nakata H, Sakamoto K, Honda Y, Mochizuki H, Hoshiyama M, and Kakigi R. Centrifugal modulation of human LEP components to a task-relevant noxious stimulation triggering voluntary movement. *Neuroimage*, 45(1): 129-42, 2009.

Nishitani N and Hari R. Viewing lip forms: cortical dynamics. *Neuron*, 36(6): 1211-20, 2002.

Noguchi Y, Inui K, and Kakigi R. Temporal dynamics of neural adaptation effect in the human visual ventral stream. *The Journal of Neuroscience*, 24(28): 6283-90, 2004.

Noguchi Y, Yokoyama T, Suzuki M, Kita S, and Kakigi R. Temporal dynamics of neural activity at the moment of emergence of conscious percept. *Journal of Cognitive Neuroscience*, 24(10): 1983-97, 2012.

Oldfield RC. The assessment and analysis of handedness: the Edinburgh inventory. *Neuropsychologia*, 9(1): 97-113, 1971.

Osipova D, Ahveninen J, Jensen O, Ylikoski A, and Pekkonen E. Altered generation of spontaneous oscillations in Alzheimer's disease. *Neuroimage*, 27(4): 835-41, 2005.

Pasley BN, Mayes LC, and Schultz RT. Subcortical discrimination of unperceived objects during binocular rivalry. *Neuron*, 42(1): 163-72, 2004.

Pelli DG. The VideoToolbox software for visual psychophysics: transforming numbers into movies. *Spatial Vision*, 10(4): 437-42, 1997.

Perrett DI, Smith PA, Potter DD, Mistlin AJ, Head AS, Milner AD, and Jeeves MA. Visual cells in the temporal cortex sensitive to face view and gaze direction. *Proceedings of the Royal Society B: Biological Sciences*, 223(1232): 293-317, 1985.

Piitulainen H, Bourguignon M, De Tiege X, Hari R, and Jousmaki V. Coherence between magnetoencephalography and hand-action-related acceleration, force, pressure, and electromyogram. *Neuroimage*, 72C: 83-90, 2013.

Pohja M, Salenius S, and Hari R. Reproducibility of cortex-muscle coherence. *Neuroimage*, 26(3): 764-70, 2005.

Proverbio AM. Tool perception suppresses 10-12Hz mu rhythm of EEG over the somatosensory area. *Biological Psychology*, 91(1): 1-7, 2012.

Proverbio AM, Adorni R, and D'Aniello GE. 250 ms to code for action affordance during observation of manipulable objects. *Neuropsychologia*, 49(9): 2711-7, 2011.

Proverbio AM, Riva F, Martin E, and Zani A. Face coding is bilateral in the female brain. *PLoS One*, 5(6): e11242, 2010.

Rizzolatti G and Matelli M. Two different streams form the dorsal visual system: anatomy and functions. *Experimental Brain Research*, 153(2): 146-57, 2003.

Rizzolatti G, Luppino G, and Matelli M. The organization of the cortical motor system: new concepts. *Electroencephalography and Clinical Neurophysiology*, 106(4): 283-96, 1998.

Rossion B, Joyce CA, Cottrell GW, and Tarr MJ. Early lateralization and orientation tuning for face, word, and object processing in the visual cortex. *Neuroimage*, 20(3): 1609-24, 2003.

Rotshtein P, Richardson MP, Winston JS, Kiebel SJ, Vuilleumier P, Eimer M, Driver J, and Dolan RJ. Amygdala damage affects event-related potentials for fearful faces at specific time windows. *Human Brain Mapping*, 31(7): 1089-105, 2010.

Sadeh B and Yovel G. Why is the N170 enhanced for inverted faces? An ERP competition experiment. *Neuroimage*, 53(2): 782-9, 2010.

Sterzer P, Jalkanen L, and Rees G. Electromagnetic responses to invisible face stimuli during binocular suppression. *Neuroimage*, 46(3): 803-8, 2009.

Suzuki M and Noguchi Y. Reversal of the face-inversion effect in N170 under unconscious visual processing. *Neuropsychologia*, 51(3): 400-9, 2013.

Tononi G and Edelman GM. Consciousness and complexity. *Science*, 282(5395): 1846-51, 1998.

Tsao DY, Freiwald WA, Tootell RB, and Livingstone MS. A cortical region consisting entirely of face-selective cells. *Science*, 311(5761): 670-4, 2006.

Tsuchiya N and Koch C. Continuous flash suppression reduces negative afterimages. *Nature Neuroscience*, 8(8): 1096-101, 2005.

Ungerleider LG and Mishkin M. Two cortical visual systems. In Ingle DJ, Goodale MA, and Mansfield RJW (Eds), *Analysis of visual behavior*. Cambridge, Massachusetts: MIT Press, 1982: 549-86.

Vingerhoets G, Alderweireldt AS, Vandemaele P, Cai Q, Van der Haegen L, Brysbaert M, and Achten E. Praxis and language are linked: evidence from co-lateralization in individuals with atypical language dominance. *Cortex*, 49(1): 172-83, 2013.

Wasaka T, Hoshiyama M, Nakata H, Nishihira Y, and Kakigi R. Gating of somatosensory evoked magnetic fields during the preparatory period of self-initiated finger movement. *Neuroimage*, 20(3): 1830-8, 2003.

Watanabe S, Miki K, and Kakigi R. Mechanisms of face perception in humans: a magneto- and electro-encephalographic study. *Neuropathology*, 25(1): 8-20, 2005.

Yokoyama T, Noguchi Y, and Kita S. Unconscious processing of direct gaze: evidence from an ERP study. *Neuropsychologia*, 51(7): 1161-8, 2013.

Table 1. Activated cerebral regions in Visible conditions (Exp. 1)

Region	BA	Hemisphere	*x*	*y*	*z*	*t*
Visible Face (150 – 230 ms)						
Intact > Random						
Lingual gyrus	19	Right	28	-72	-6	5.11
Middle temporal gyrus	39	Right	54	-80	30	11.37
Inferior parietal lobule	40	Right	40	-34	30	6.36
Inferior parietal lobule	40	Left	-66	-44	42	5.51
Superior temporal gyrus	38	Left	-44	12	-8	5.39
Visible Tool (350 – 450 ms)						
Intact > Random						
Supramarginal gyrus	40	Left	-54	-44	34	4.68
Superior temporal gyrus	42	Left	-74	-30	16	4.49
Superior parietal lobule	7	Left	-38	-68	50	4.35
Cuneus	17	Left	0	-96	-4	4.24
Anterior cingulate	32	Left	-18	32	12	9.04
Middle Occipital Gyrus	18	Left	-38	-98	10	7.27
Medial frontal gyrus	9	Left	0	50	26	5.63
Supramarginal gyrus	40	Right	42	-40	36	7.63
Superior temporal gyrus	22	Right	74	-40	14	4.51
Superior temporal gyrus	38	Right	52	14	-8	7.27
Cuneus	17	Right	26	-80	8	7.65

BA. Brodmann's area near the coordinates

Table 2. Activated cerebral regions in Invisible conditions (Exp. 2)

Region	BA	Hemisphere	*x*	*y*	*z*	*t*
Invisible Tool (650 – 750 ms)						
Intact > Random						
Inferior Parietal lobule	39	Left	-42	-72	40	7.35
Posterior cingulate	31	Left	-24	-60	12	9.97
Middle frontal gyrus	10	Left	-42	62	16	6.22
Middle occipital gyrus	18	Left	-22	-94	0	4.65
Inferior parietal lobule	40	Right	42	-40	50	5.02
Middle temporal gyrus	19	Right	58	-76	16	9.56

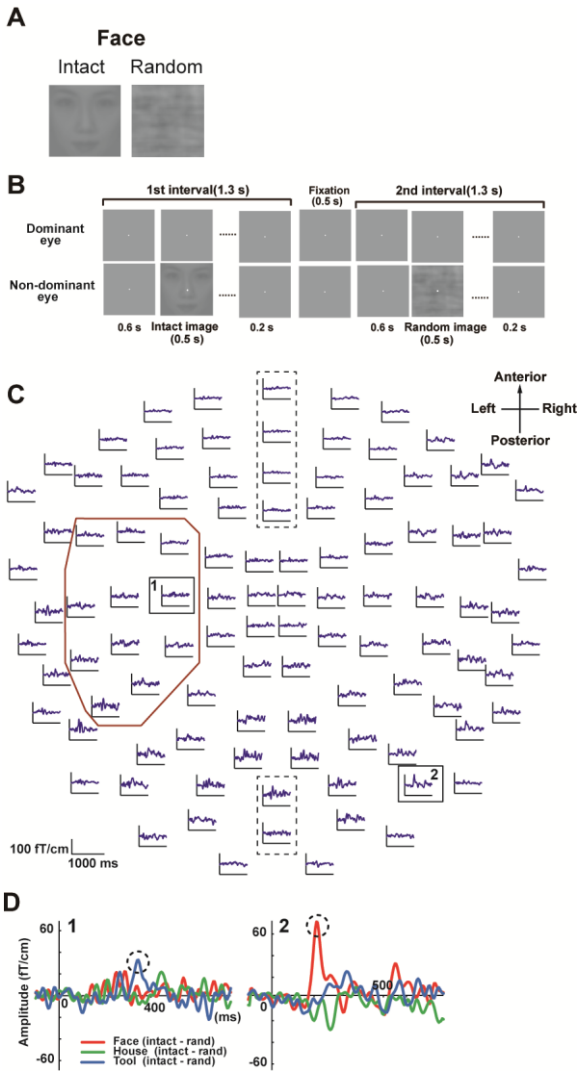

Figure 1. Experiment 1. **(A)** Six types of object images. For each of three categories (face, house and tool), intact and random (scrambled) images were prepared. **(B)** A structure of one trial. Every trial consisted of two intervals of 1.3 s. An intact object image (face, house or tool) was presented to a non-dominant eye of subject in either the first or second interval, while its random image appeared in the other. We presented a gray image with a fixation to a dominant eye so that subjects could consciously perceive the object images to the non-dominant eye. At the end of every trial, subjects reported a category of the intact image, ignoring the random image. **(C)** Visual-evoked fields (VEFs) at 102 sensor positions of MEG. Differential (intact - random) waveforms to the face images in a representative subject are shown. The data in two types of trials (first-intact/second-random trials and

first-random/second-intact trials) were pooled (see **Supplementary Fig. S3** for an effect of a stimulus sequence). The waveforms recorded from anterior regions are plotted in the upper positions. Six sensors on the midline position (dotted rectangles) were excluded from the sensor of interest (SOI) analyses (see **Methods**). The data at 11 sensors encompassed by red lines were used for frequency analyses (see **Fig. 5**). **(D)** Enlarged VEFs in two sensors (1 and 2) in panel **C.** Neuromagnetic responses to faces, houses, and tools are shown in red, green, and blue lines, respectively.

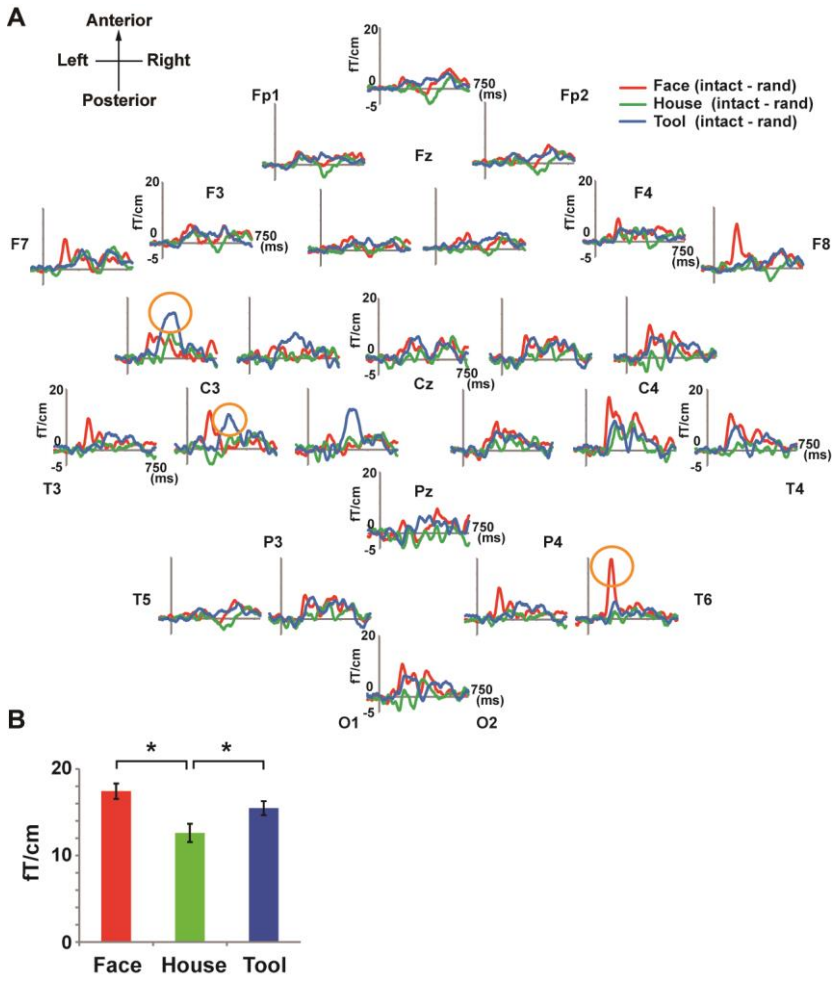

Figure 2. Neuromagnetic responses for visible objects. **(A)** Averaged VEFs across 11 subjects in 26 groups of sensors. We divided differential (intact – random) VEFs at all 102 sensor positions into 26 groups (see **Methods**). The VEFs belonging to the same group were averaged together. Large VEFs for visible face images (red) were seen in the right-posterior region, while visible tool images (blue) induced strong neural responses in the left hemisphere (orange circles). As a rough indication for positions of each sensors group on the scalp, we placed labels of EEG electrodes in the international 10-20 system (although no EEG signals were measured actually). (B) Peak amplitudes of VEFs averaged over 26 groups. Error bars denote SE across 11 subjects. The VEFs induced by house images were smaller than those induced by face and tool images. * $p < .05$.

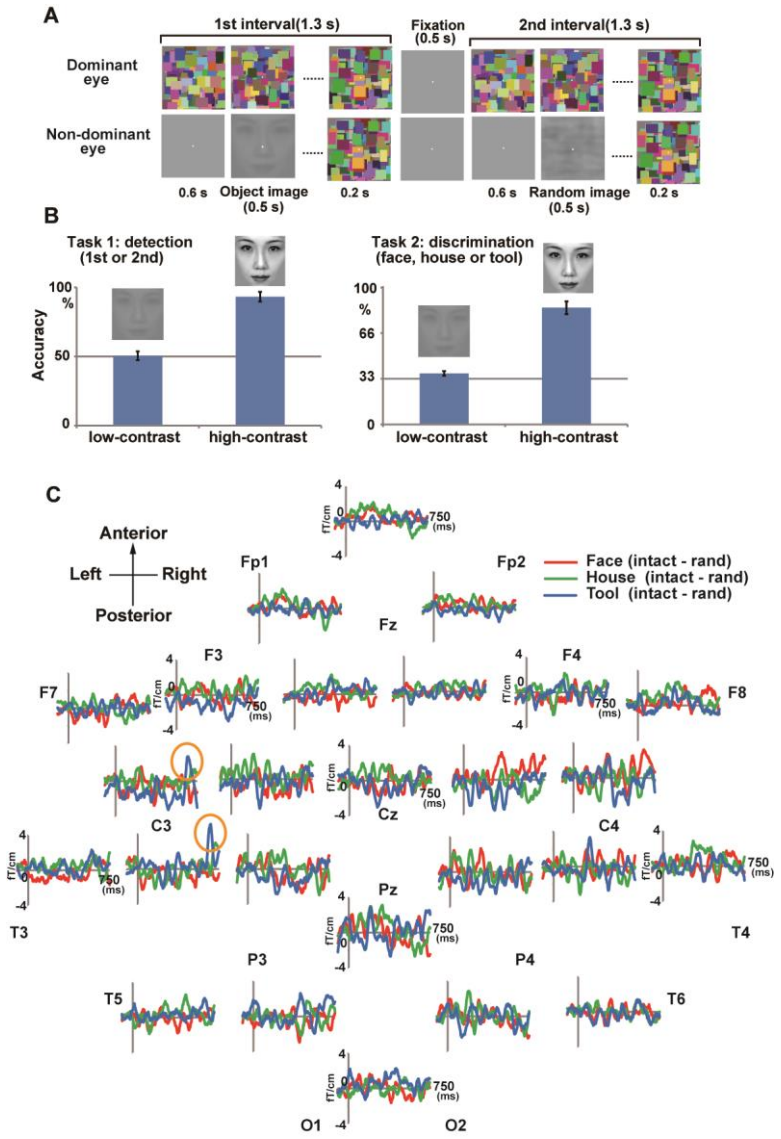

Figure 3. Experiment 2. **(A)** A sequence of one trial. Basic structures were identical to Experiment 1 except that a conscious perception of object images was prevented by continuous flashes presented to dominant eye of subjects. At the end of each trial, subjects performed two tasks. The first task asked an interval (first or second) which contained an intact object image (2AFC detection task). Subjects then reported a category (face, house, or tool) of the intact image (discrimination task). **(B)** Behavioral results of the two tasks. Error bars denote standard errors (SEs) across 11 subjects. For low-contrast object images, the detection (task 1) and discrimination (task 2) rates were not significantly different from the chance-levels of each task (task 1: 50 %, task 2: 33 %), indicating that those low-contrast images were kept invisible in Experiment 2. Conversely, subjects perceived high-contrast

images consciously even under CFS. **(C)** Averaged VEFs in 26 groups to the low-contrast (invisible) images. Neuromagnetic signals to those invisible images were strongly suppressed compared to visible images (note a difference in the vertical scale from **Fig. 2A**). Nevertheless, distinct responses to tool images were observed in the left hemisphere (orange circles).

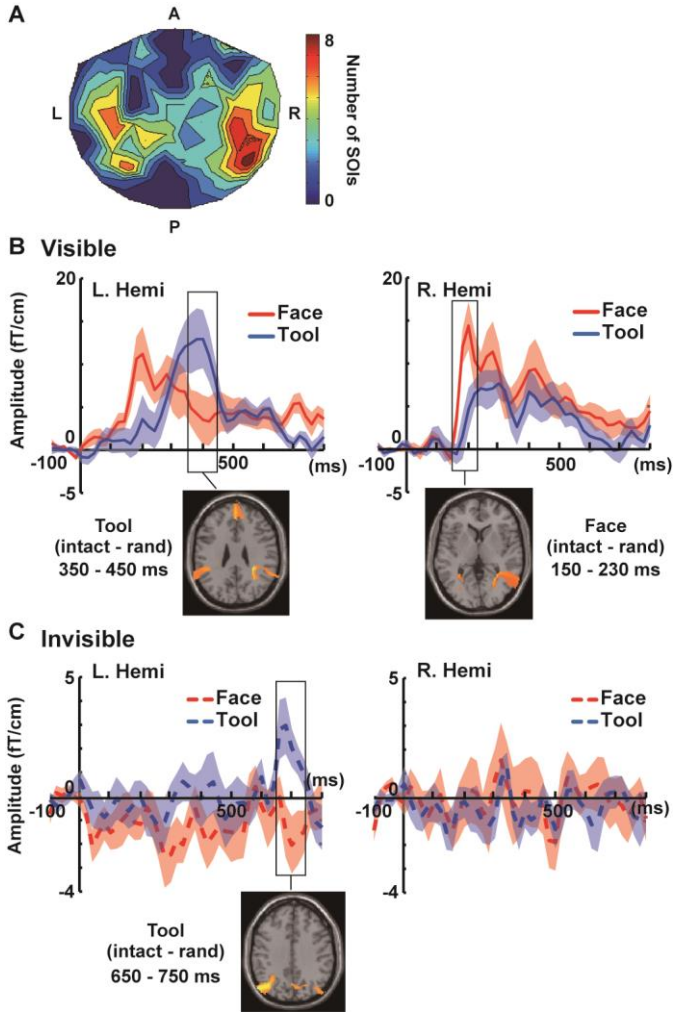

Figure 4. The sensor of interest (SOI) analyses. **(A)** The distribution of SOIs across 11 subjects. The number of selected sensors in each position was summed across subjects and color-coded on a contour map depicted over the topographical layout of 102 sensor positions. **(B)** Across-SOI VEFs of the visible condition (Exp. 1) in the left and right hemispheres. Red and blue lines indicate responses to faces and tools, respectively. Background shadings denote SE across 11 subjects. The results of source estimations using the MSP analyses (see **Methods**) are also shown in insets. Position of axial slice are z = 28 (left panel) and z = 4 (right panel) in MNI coordinates. (C) Across-SOI VEFs in the invisible condition (Exp. 2). Position of axial slice in the inset is z = 36.

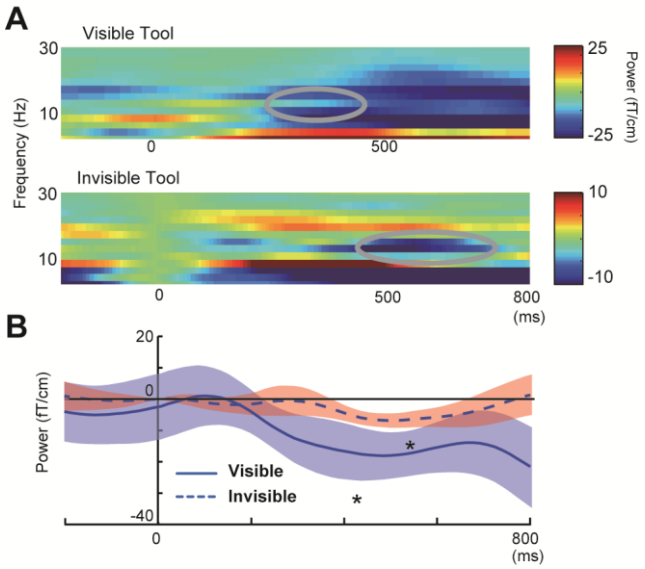

Figure 5. Results of frequency analyses. **(A)** Power spectra of MEG waveforms (averaged across 11 subjects) to visible and invisible tool images in the left hemisphere. A suppression of upper μ rhythm (11 – 13 Hz), a neural index of motor execution and imagery, was observed when visible tool images were presented (a gray circle in an upper panel). A similar desynchronization was also seen to invisible tools (lower panel) but in a later time window around 500 ms. **(B)** Temporal changes of the power in 11 -13 Hz for visible (solid) and invisible (broken) tool images. Background shadings denote SE across the 11 subjects. The asterisks (*) indicate significant ($p < .05$) deflections from the baseline period (see **Results**).